Available online at www.sciencedirect.com
SCIENCE DIRECT
Polymer 46 (2005) 8546–8554
polymer
www.elsevier.com/locate/polymer

Multiblock copolymers synthesized in aqueous dispersions using multifunctional RAFT agents

Raf Bussels[a], Christianne Bergman-Göttgens[a], Jan Meuldijk[b], Cor Koning[a,*]

[a]*Laboratory of Polymer Chemistry, Eindhoven University of Technology, P.O. Box 513, 5600 MB Eindhoven, The Netherlands*
[b]*Process Development Group, Eindhoven University of Technology, P.O. Box 513, 5600 MB Eindhoven, The Netherlands*

Received 25 November 2004; accepted 2 February 2005
Available online 13 June 2005

Abstract

Triblock copolymers were synthesized in aqueous dispersions in two polymerization steps using a low molar mass difunctional dithiocarbamate-based RAFT agent, and in merely one polymerization step using a macromolecular difunctional dithiocarbamate-based RAFT agent. Segmented block copolymers containing several alternating blocks of different polarities were synthesized in miniemulsion in merely two polymerization steps by applying multifunctional, dithiocarbamate-based RAFT agents. All polymerizations showed a linear increase of $\bar{M}_n$ with monomer conversion. Evidence that this novel synthetic concept resulted in the formation of (multi)block copolymers was obtained by combining normal gel permeation chromatography with gradient polymer elution chromatography.

Keywords: RAFT polymerization; Dithiocarbamates; Miniemulsion

1. Introduction

Reversible addition fragmentation chain transfer (RAFT) radical polymerization can be regarded as the most versatile, the most robust, and accordingly the most promising 'living' radical polymerization technique [1,2]. Both polar and non-polar monomers can be polymerized by this technique, and living polymerizations can be performed under a broad range of reaction conditions, both in solution and in aqueous dispersions [1–8].

Other research groups have demonstrated that the RAFT polymerization technique allows the synthesis of (multi)-block copolymers [9], even in aqueous dispersions [10–12]. However, for the manufacturing of a multiblock copolymer, consisting of n polar and m non-polar blocks, $(n+m)$ separate monomer additions are required if a standard monofunctional RAFT agent is used.

In this paper, the miniemulsion polymerization of acrylic monomers mediated with multifunctional *S*-*tert*-alkyl-*N*,*N*-alkoxycarbonylmethyldithiocarbamate RAFT agents (Scheme 1) is discussed. If in this type of RAFT agent the nitrogen atoms are part of an aromatic system, or bound to electron-withdrawing groups, the resulting dithiocarbamates are effective RAFT agents [13–15].

Scheme 1 shows the RAFT agents that are used in this paper. The synthesis of these compounds has been described elsewhere [16]. Using the difunctional 'butyl-RAFT' agent, it is possible to synthesize triblock copolymers in two polymerization steps, while employing the difunctional 'Kraton-RAFT' agent (based on 'Kraton-L1203', which is a mono hydroxyl end capped poly(ethylene-*co*-butylene) with an $\bar{M}_n$ of 4000 g/mol and a polydispersity index of 1.02) allows the synthesis of a triblock copolymer in merely one polymerization step [16]. The multifunctional 'poly(decyl)-RAFT' agent ($\bar{M}_n = 3700$ g mol^{-1}, PDI = 1.59) depicted in Scheme 1 provides multiblock copolymers in merely two sequential polymerization steps [16]. The 'poly(decyl-RAFT)' used in this study contains an average number of twelve RAFT moieties per molecule.

Although the general concept of monomer insertion into polymer chains by controlled radical polymerization is not new [17–19], the versatile route described here is different and novel. This paper shows that the new dithiocarbamate-based RAFT agents are able to mediate radical polymerizations in

* Corresponding author. Tel.: +31 40 2472840; fax: +31 40 2463966.
E-mail address: c.e.koning@tue.nl (C. Koning).

0032-3861/$ - see front matter © 2005 Elsevier Ltd. All rights reserved.
doi:10.1016/j.polymer.2005.02.126

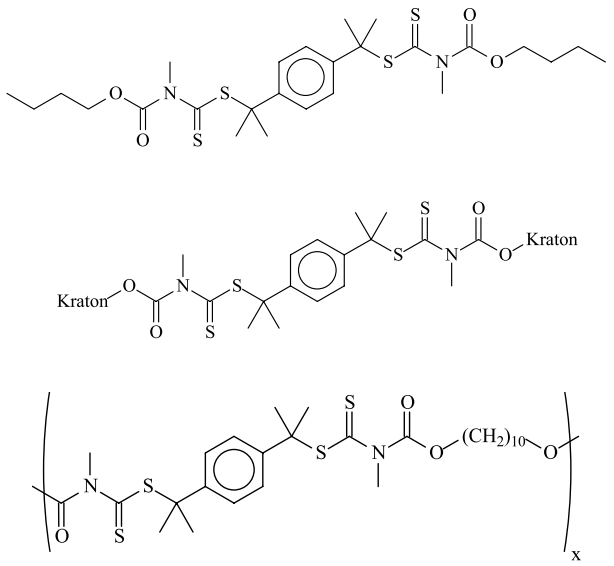

Scheme 1. *S*-(1,4-Phenylenebis(propane-2,2-diyl)bis(*N*,*N*-butoxycarbonyl-methyldithiocarbamate)) and *S*-(1,4-phenylenebis(propane-2,2-diyl)bis(*N*, *N*-'Kraton'carbonyl-methyldithiocarbamate)), and poly(*S*-(1,4-phenylene-bis(propane-2,2-diyl)) bis(*N*,*N*-decoxycarbonylmethyldithiocarbamate)), respectively, the difunctional 'butyl-RAFT' and 'Kraton-RAFT' agents, and the multifunctional 'poly(decyl-RAFT)' agent.

such a way that $\bar{M}_n$ increases linearly with conversion. The generated (multi)block copolymers, directly applicable in the form of environmentally benign latexes as e.g. pressure sensitive adhesives, may be even based on commercially available hydroxyl end capped polymers, like e.g. the mentioned highly non-polar 'Kraton-L1203'.

2. Experimental

2.1. Materials

All solvents used were purchased from Biosolve BV, and were dried and purified before use in a Grubbs column, except for methanol and dichloromethane, which were used as received. All other chemicals were obtained from Aldrich and used without further purification. Kraton L-1203 was used as received from the manufacturer Kraton BV (see section 1 for a description). The synthesis of the RAFT agents has been described elsewhere [16].

2.2. Polymerizations

For the miniemulsion polymerizations using the 'butyl-RAFT' agent, 4.4×10^{-2} mol 'butyl-RAFT' per $L_{organic\ phase}$ was dissolved under stirring in a mixture of 8.0 g *n*-butyl acrylate (*n*BA) monomer and 2 wt% hexadecane (with respect to *n*BA), comprising the organic phase. In the aqueous phase (30 g water), 2.3×10^{-3} mol sodium dodecyl sulphate (SDS) was present per L_{water}. The organic phase was added dropwise to the aqueous phase under vigorous stirring. The pre-emulsion was sonicated for 30 min. After emulsification, the miniemulsion was transferred into a jacketed reactor under argon atmosphere. The reactor was equipped with a reflux cooler and a thermocouple. The miniemulsion was heated to 70 °C under stirring, and an aqueous solution, containing the required amount of KPS to obtain an initial KPS concentration of 3.0×10^{-3} mol/L_{water}, was added, after which polymerization was performed for 3 h. For all polymerizations, at regular time intervals, samples were taken for gravimetric conversion measurement and GPC analysis, using PS standards.

The poly(*n*-butyl acrylate) latex obtained after the described polymerization (=formation of the first block), was applied as a seed latex for the polymerization of the second monomer. Fifteen grams of the poly(*n*BA) latex was swollen overnight at room temperature with 3.0 g of *iso*-octyl acrylate (*i*OA). Then, the second polymerization step was performed under argon, under the same conditions as described for the first step, using fresh KPS. [KPS]$=3.0\times10^{-3}$ mol/L_{water}.

For the miniemulsion polymerizations using the 'Kraton-RAFT' agent, the following conditions were used. Polymerization time: 3 h at 70 °C. Organic phase: 2.0 g 'Kraton-RAFT' agent, 8.0 g *n*BA, 2 wt% hexadecane with respect to *n*BA. Aqueous phase: 30 g water, with [SDS]$=4.6\times10^{-3}$ mol/L_{water} and [KPS]$=3.0\times10^{-3}$ mol/L_{water}. In one special case, 4 g of *n*BA was replaced with 4 g of toluene, which was used as co-solvent for the 'Kraton-RAFT' agent. This is described in detail in Section 3 of this paper.

The RAFT polymerizations, using the multifunctional 'poly(decyl-RAFT)' agent, were performed under the same conditions as described above for the difunctional 'butyl-RAFT' agent. Conditions: 3 h, 70 °C; organic phase: 8.0 g *n*BA, 2 wt% hexadecane with respect to *n*BA, 8.0×10^{-3} mol 'poly(decyl-RAFT)' per $L_{organic\ phase}$. Aqueous phase: 30 g water, 2.3×10^{-3} mol sodium dodecyl sulphate (SDS) per L_{water}, 2.5×10^{-3} mol potassium peroxodisulphate (KPS) per L_{water}.

The poly(*n*BA) latex, obtained in the miniemulsion polymerization with the 'poly(decyl-RAFT)' agent described above, was used as a seed latex for the emulsion polymerization of *iso*-octyl acrylate (*i*OA). For this seeded emulsion polymerization the conditions were similar to those used for the seeded emulsion polymerization described for the 'butyl-RAFT' agent (see above).

2.3. Methods and equipment

GPC analysis was carried out using a Waters model 510 pump, a model 410 refractive index detector (at 40 °C) and a model 486 UV detector (at 254 nm) in series. Injections were done by a Waters model WISP 712 autoinjector, using an injection volume of 50 μL. The columns used were a PLgel guard (5 μm particles) 50×7.5 mm^2 column, followed by two PLgel mixed-C or mixed-D (5 μm particles)

300×7.5 mm columns at 40 °C in series. Tetrahydrofuran (Biosolve, stabilised with BHT) was used as eluent at a flow rate of 1.0 mL min^{-1}. Calibration has been done using polystyrene standards (Polymer Laboratories, $\bar{M}_n = 580 - 7.1 \times 10^6$ g mol^{-1}). Data acquisition and processing were performed using Waters Millennium32 (version 3.2 or 4.0) software. Before injection, the samples were filtered over a 13 mm×0.2 μm PTFE filter, PP housing (Alltech).

Molar mass and chemical composition distribution (MMCCD) determination was carried out in two steps. In a first step, GPC fractionation was carried out using a Separations model Gyncotek P580 isocratic pump, a Viscotek 250 dual detector (DRI and viscometer, but only the 250 DRI detector was used) 250 DRI detector, and a Spectra Physics Linear™ UV–vis detector (operated at 254 nm), in series. Injections were done by a Separations model MIDAS autoinjector, using an injection volume of 50 μL. The columns used were a PLgel guard (5 μm particles) 50×7.5 mm column, followed by two PLgel mixed-D 5 μm columns, a PLgel Mixed-C 5 μm column and a PLgel Mixed-B 10 μm column in series (Polymer Laboratories). Tetrahydrofuran (Biosolve, stabilised with BHT) was used as eluent at a flow rate of 1.0 mL min^{-1}. A fraction collector (Millipore) was used to collect 47 fractions at equal volume intervals of nine droplets. A solution of the polymer in THF was injected 20 times and the corresponding fractions were collected. All 47 fractions were reinjected on the SEC system after fractionation. In a second step, GPEC analysis was carried out on an Agilent Technologies 1100 series system, using a G1311A quaternary pump, a G1313A autosampler, a G1315B UV-DAD detector at 254 nm and a S.E.D.E.R.E France SEDEX 55 ELSD detector, operated at 2.2 bar and 60 °C. All data were processed with HP Chemstation software. The column used was a Zorbax Eclipse SDB-C18 4.6×150 mm column, using a THF (HPLC grade, Biosolve)/water 85:15 to THF gradient in 20 min at a flow of 1.0 mL min^{-1} at 25 °C. Samples were dissolved in THF (HPLC grade, Biosolve) at a concentration of 10 mg mL^{-1}. Before gradient polymer elution chromatography (GPEC) analysis, the solvent in the samples obtained via GPC fractionation was evaporated to such an extent that approximately a ten-fold increase of the polymer concentration in the fractions was obtained. The injection volume was 10 μL.

For the cryo-TEM analysis, the samples were prepared using a Vitrobot® vitrification robot, in which the relative humidity is kept close to saturation to prevent water evaporation from the sample [www.vitrobot.com]. A 3 μL drop of the solution was placed on a carbon-coated lacy substrate supported by a TEM 300 mesh copper grid (Ted Pella). After automatic blotting with filter paper, in order to create a thin liquid film over the grid, the grid was rapidly plunged into liquid ethane at its melting temperature. This resulted in a vitrified film. The vitrified specimen was then transferred under a liquid nitrogen environment to a cryo-holder (model 626, Gatan Inc., Warrendale, PA) into the electron microscope, Tecnai 20-Sphera (FEI), operating at 200 kV with a nominal underfocus of 2–4 μm. The working temperature was kept below −175 °C, and the images were recorded on a Gatan 794 MultiScan digital camera and processed with Digital Micrograph 3.6.

Particle diameters were measured on an LS 32 Coulter Counter. For this purpose, samples were diluted with deionized water.

3. Results and discussion

3.1. Polymerizations mediated with the 'butyl-RAFT' agent

The solubility of the 'butyl-RAFT' agent in *n*BA was excellent, and this solution remained homogeneous during the preparation of the miniemulsion under high shear conditions. Fig. 1 shows the linear increase of $\bar{M}_n$ with *n*-butyl acrylate (*n*BA) conversion, which is a good indication that the addition of the 'butyl-RAFT' agent provided control of the radical polymerization, and that the number of growing chains was constant. The measured values for $\bar{M}_n$ are somewhat higher than the calculated values, which cannot be explained by the fact that these are expressed in polystyrene equivalents, since the Mark–Houwink–Sakurada constants of polystyrene and poly(*n*BA) are quite similar. However, one should realize that the synthesized macromolecules are not pure poly(*n*BA). The relatively low molar mass polymer molecules are end capped with sulphur-containing 'butyl-RAFT' residues, which may influence the Mark–Houwink–Sakurada constants. Also termination of a RAFT function may occur, which will reduce the number of RAFT functions, and thus increase the number-average molar mass. Finally, exit of growing radical chains (which still contain one dormant RAFT function) from the latex particles cannot be excluded. A comment on the relatively high PDI values will be given at the end of Section 3.

In another miniemulsion polymerization experiment, 10 wt% of the *n*BA monomer was successfully substituted

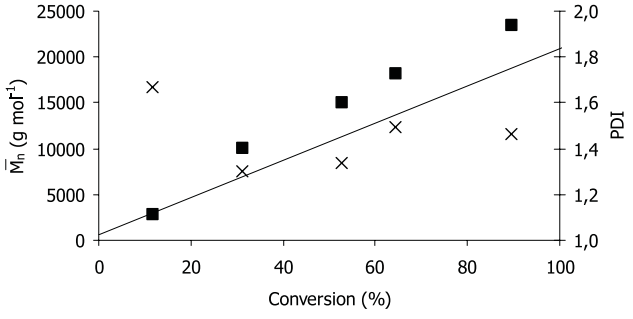

Fig. 1. Number average molar mass ($\bar{M}_n$, ■) and polydispersity index (PDI, ×) versus conversion for the miniemulsion polymerization of *n*-butylacrylate (*n*BA), using the 'butyl-RAFT'agent. Drawn line is theoretical $\bar{M}_n$. Average particle diameter after polymerisation: 174 nm.

by the highly polar methacrylic acid (MAA), leaving the rest of the variables exactly the same. For this polymerization, the theoretical and experimental $\bar{M}_n$ were 20,100 and 22,500 g/mol, respectively, and the polydispersity index after 92% conversion was 1.48. So, relatively polar blocks with a controlled length can be synthesized using this new concept. The amount of incorporated MAA was determined via GPEC and potentiometric titrations, and was shown to be slightly higher than expected from the overall molar MAA/*n*BA ratio. The reason for this is that MAA is more reactive than *n*BA, and that the overall monomer conversion was only 80%.

The poly(*n*BA) latex described above was applied as a seed latex for the polymerization of the second monomer *iso*-octyl acrylate (*i*OA). The poly(*n*BA) in this seed latex had a $\bar{M}_n$ of 23,500 g/mol after 90% monomer conversion (Fig. 1). For this seeded emulsion polymerization, yielding a triblock copolymer, $\bar{M}_n$ increases linearly with *i*OA conversion, see Fig. 2. In this case the deviation between theoretical and experimental $\bar{M}_n$ is expected in view of the PS calibration and the presence of poly(*i*OA) blocks in the copolymer. Of course the other possible reasons for the deviation, given above, remain valid.

3.2. Polymerizations mediated with the 'Kraton-RAFT' agent

Fig. 3 shows the SEC chromatogram of the miniemulsion RAFT polymerization of *n*BA, mediated with the difunctional 'Kraton-RAFT' as the mediating agent. For this polymerization, the conditions and concentrations were identical to those used for the living radical polymerization of *n*BA using the difunctional 'butyl-RAFT' agent. After polymerization, a significant part of the 'Kraton-RAFT' agent proved to be unreacted (peak at an elution time of 15 min). Furthermore, high molecular weight, uncontrolled poly(*n*BA) is found (broad peak at elution times from 8 to 12 min). Clearly, no control over the polymerization was achieved.

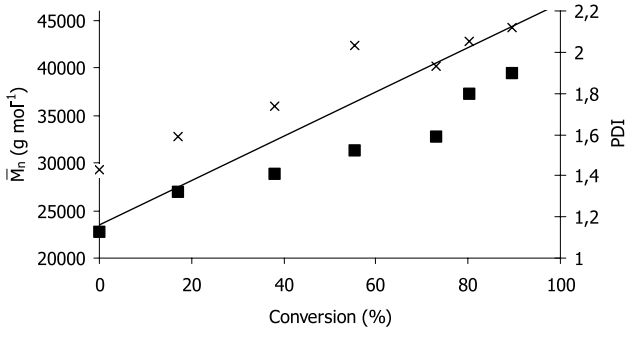

Fig. 2. Number average molar mass ($\bar{M}_n$, ■) and polydispersity index (PDI, ×) versus conversion for the seeded emulsion polymerization of *iso*-octyl acrylate (*i*OA) on the poly(*n*BA) seed latex, prepared using the 'butyl-RAFT'agent. Drawn line is theoretical $\bar{M}_n$. Average particle diameter after polymerization: 205 nm.

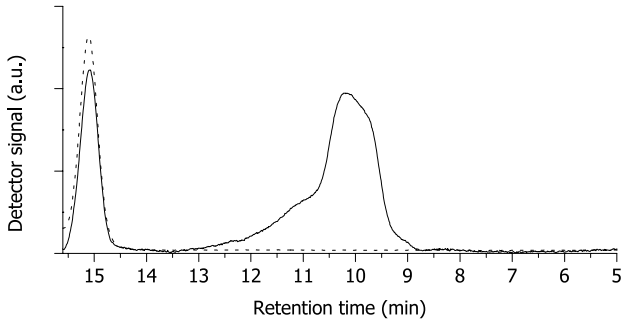

Fig. 3. Normalized molecular weight distribution of the miniemulsion RAFT polymerization of *n*BA mediated with the 'Kraton-RAFT' agent before (- - -) and after (—) polymerization. Average particle diameter after polymerization: 131 nm.

In order to study the lack of control over the *n*BA polymerization mediated with the 'Kraton-RAFT' agent, latex samples, as well as samples of the miniemulsion before polymerization were studied with cryo-TEM. In Figs. 4 and 5, cryo-TEM pictures before (Fig. 4) and after (Fig. 5) polymerization are depicted. The large, light grey vitrified water droplets contain darker latex particles. Fig. 4 reveals the presence of two types of particles in the miniemulsion before polymerization: sharply bordered particles ($\bar{D}_n$ = 20 nm) and large, vaguely bordered particles ($\bar{D}_n$ = 300 nm). Clearly the vaguely bordered particles are dominant, while the sharply bordered particles are sparse. On the cryo-TEM pictures taken after polymerization of the miniemulsion, these same two types of particles can be discerned, although the number ratio and the size of the particles has changed: the vaguely bordered particles ($\bar{D}_n$ = 350 nm) and the sharply-bordered latex particles ($\bar{D}_n$ = 100 nm) are present in a 2:3 ratio. The vaguely bordered particles tend to coagulate here, while in the sample before polymerization the vaguely bordered particles were isolated. The existence of such vaguely bordered particles in a latex has been reported by Almgren et al. [20] for emulsions of fine oil droplets with lecithin as emulsifier, and were designated 'unidentified fatty objects'. From the variation of the contrast these authors concluded that these objects were lens shaped, and oriented face on, presumably at the water/air interface. They suggested that oil droplets without emulsifier would form such lenses at the air/water interface. The existence of two types of particles after the polymerization strongly suggests that microphase separation has occurred in the latex particles, either during the polymerization, or during the miniemulsion preparation. In Table 1, the properties and the most likely composition of each type of particle are summarized. Since the latex was polymerized above the upper critical solution temperature (UCST, which we determined to be 28 °C for a mixture of 'Kraton-RAFT' agent and *n*BA in a 20:80 ratio), microphase separation during the polymerization seems unlikely, and therefore is assumed to have occurred during the miniemulsion preparation.

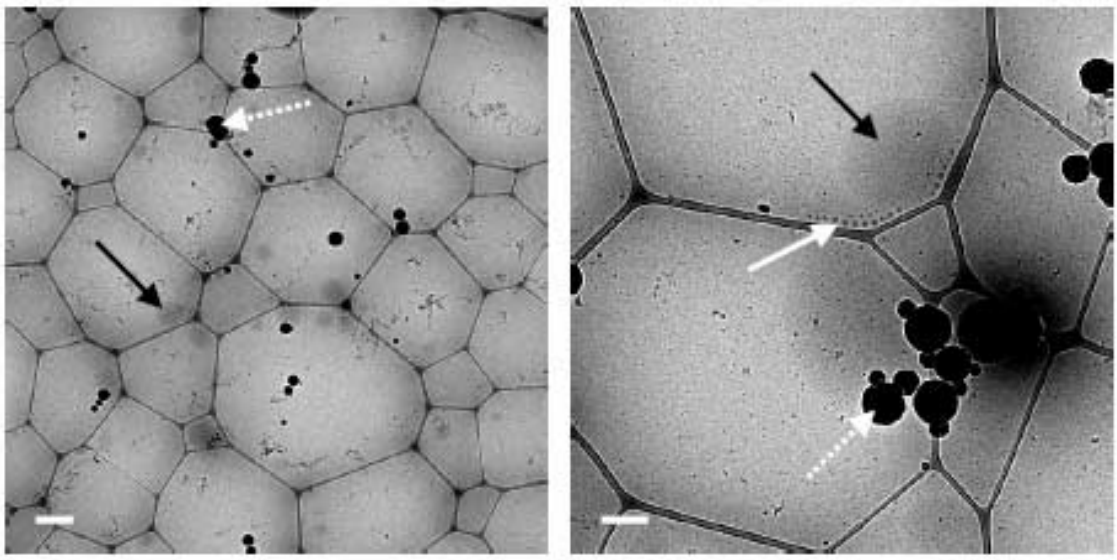

Fig. 4. Cryo-TEM pictures taken before polymerization. Inside the light grey vitrified water droplets, sharply bordered miniemulsion droplets can be observed ($\bar{D}_n = 20$ nm, white thick arrow) together with vaguely bordered, lens-shaped particles ($\bar{D}_n = 300$ nm, black thick arrow). The black particles (white dashed arrow) are ice crystals. (a) Bar = 200 nm. (b) Bar = 100 nm.

As a result of the high local energy and shear, originating from the ultrasound waves, which intensify the dynamic process of break-up and coalescence of the 'Kraton-RAFT' agent containing *n*BA droplets, some water is introduced into these droplets. As a consequence the 'Kraton-RAFT' agent immediately precipitates and becomes unavailable for controlling the radical polymerization of *n*BA. Note that the solubility of the 'Kraton-RAFT' agent in *n*BA decreases dramatically upon the addition of traces of water. Redissolution does not occur after increasing the temperature above the UCST, i.e. 28 °C for a mixture containing 20 wt% 'Kraton-RAFT' and 80/wt% *n*BA. This result supports the hypothesis for the lack of control of the *n*BA polymerization. The small 20 nm droplets have probably been formed after the precipitation of the 'Kraton-RAFT' agent, and do not contain any 'Kraton-RAFT'. The large particles that can

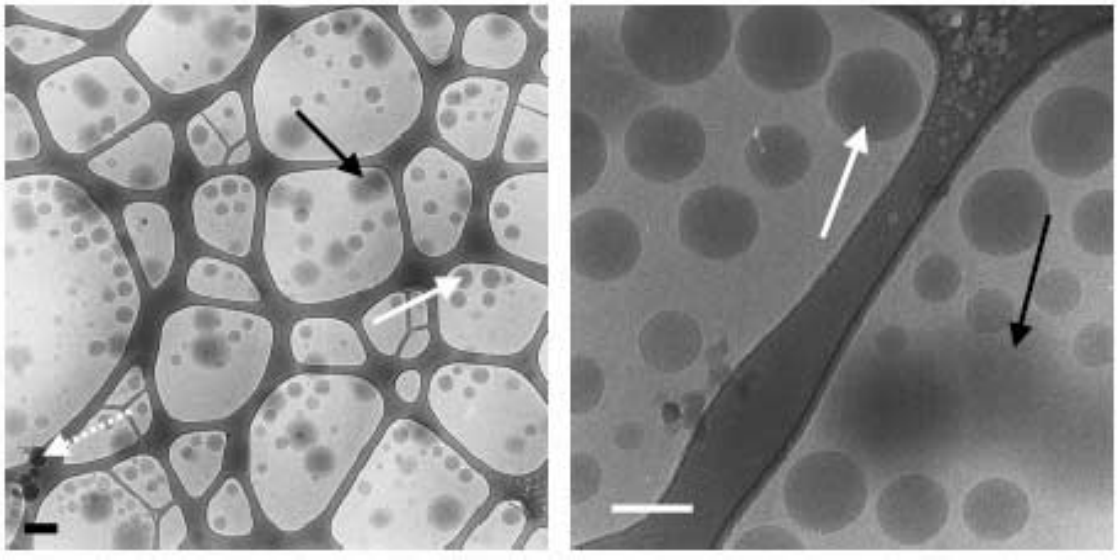

Fig. 5. Cryo-TEM pictures taken after polymerization. Inside the light grey vitrified water droplets, sharply bordered latex particles can be observed ($\bar{D}_n = 100$ nm, white thick arrow) together with vaguely bordered, lens-shaped particles ($\bar{D}_n = 350$ nm, black thick arrow). The black particles (white dashed arrow) are ice crystals. (a) Bar = 200 nm. (b) Bar = 100 nm.

Table 1
Properties and assumed composition of the two types of particles observed in the cryo-TEM pictures of an *n*BA miniemulsion polymerization mediated with the 'Kraton-RAFT' agent, before and after polymerization

Particle type	Before polymerization (Fig. 4)			After polymerization (Fig. 5)		
	Abundance[a]	$\bar{D}_n$ (nm)	Composition	Abundance[a]	$\bar{D}_n$ (nm)	Composition
Lens-shaped particles	Dominant	300	*n*-BA hexadecane 'Kraton-RAFT' agent	Fair−	350	Hexadecane 'Kraton-RAFT' agent
Sharply bordered particles	Sparse	20	*n*-BA hexadecane	Fair+	100	p(*n*-BA) hexadecane

[a] The denotations dominant > fair+ > fair− > sparse indicate a decreasing relative abundance of the specific particle type.

be observed in Fig. 4 are most likely the miniemulsion droplets containing the collapsed 'Kraton-RAFT' agent. Once the polymerization has been initiated, the probability for radicals to enter the small, sharply bordered *n*BA containing particles [Fig. 4(b)] is much larger than for radical entry in the lens-shaped particles, since the total surface area of the sharply bordered particles with an average particle diameter of 20 nm is much larger than that of the lens-shaped particles. During the polymerization, monomer transport occurs from the large miniemulsion droplets to the very small, sharply bordered particles, where non-controlled free radical polymerization proceeds. During this polymerization, the sharply bordered particles grow as in a conventional emulsion polymerization, and uncontrolled polymer is formed inside these particles, because these do not contain mediating RAFT agent. This mechanism explains the sparseness and the size of the sharply bordered particles in the miniemulsion before polymerization (Fig. 4), while after polymerization, more and larger latex particles are present in the latex than lens-shaped particles, which is in agreement with the miniemulsion recipe.

Phase separation in the 'Kraton-RAFT'/*n*BA system could be avoided by replacing 50 wt% of *n*BA by toluene, which is a good solvent for the 'Kraton-RAFT' agent. In this miniemulsion polymerization experiment, a stable latex was obtained, and as for the 'butyl-RAFT' agent $\bar{M}_n$ increases linearly with *n*BA conversion, see Fig. 6. The difference between calculated and experimental $\bar{M}_n$ is expected in view of the PS calibration and the presence of poly(ethylene-*co*-butylene) blocks in the copolymer. However, in addition termination of a RAFT function may occur, reducing the number of RAFT functions, and thus increasing the number-average molar mass.

The GPC traces of the product obtained in this experiment clearly show the shift of the 'Kraton-RAFT' agent to higher molecular weight, indicating that incorporation of the monomer occurred, see Fig. 7.

Theoretically, the polymerization using the 'Kraton-RAFT'agent yields a triblock copolymer in merely one polymerization step, with a poly(*n*BA) block in the middle and Kraton blocks at both ends. However, from the GPC chromatograms shown in Fig. 7 it may appear that upon polymerization not all initially present RAFT agent (eluting after 15 min) was consumed. To check this, a full MMCCD determination was performed (GPC–GPEC), which revealed that all initial 'Kraton-RAFT' agent was consumed, but also that some diblock copolymer had been formed (compound C in Fig. 8). This can be attributed to radical termination of one of the RAFT functions on the 'Kraton-RAFT' agent, after which only two blocks remain in the polymer chain. This side reaction can also explain the relatively broad molar mass distribution, plotted in Fig. 6. Moreover, after synthesis, the 'Kraton-RAFT' agent was used without purification. So, possible impurities, like the coupling product of a dithiocarbamate molecule and only one molecule of Kraton-chloroformate, were not removed. This product would also yield a diblock instead of the

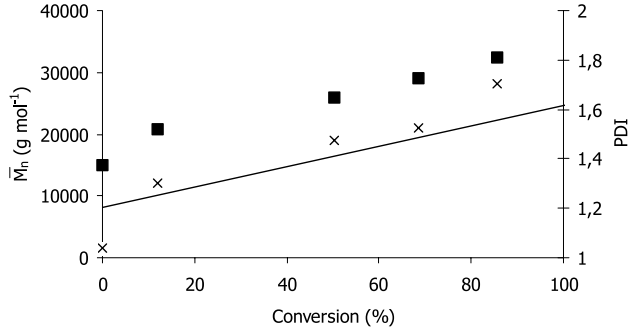

Fig. 6. Number average molar mass ($\bar{M}_n$, ■) and polydispersity index (PDI, ×) versus conversion for the miniemulsion polymerization of *n*BA, diluted with 50% toluene, using the difunctional 'Kraton-RAFT'agent. Drawn line is theoretical $\bar{M}_n$.

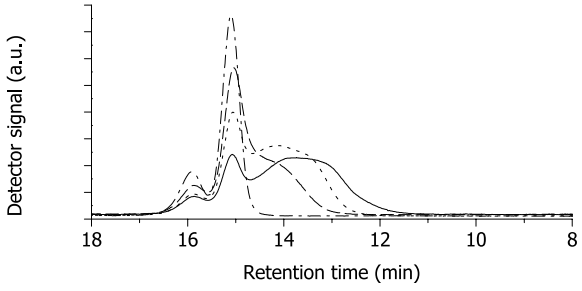

Fig. 7. Normalized GPC chromatograms of the 'Kraton-RAFT'-mediated miniemulsion polymerization with 50:50 toluene/*n*BA. No conversion (– – – – –); 12% monomer conversion (– – –); 50% monomer conversion (- - -); 86% monomer conversion (—). Average particle size after polymerization: 142 nm.

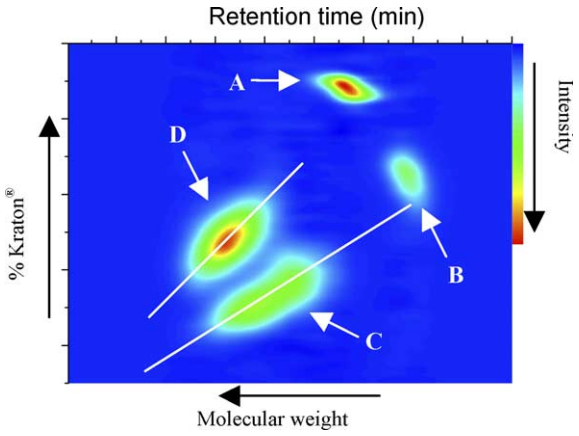

Fig. 8. GPEC–GPC separation plot of the reaction mixture of the polymerization of *n*BA, using 'Kraton-RAFT'. A = di(Kraton)carbonate; B = Kraton chloroformate; C = Kraton-*b*-poly(*n*BA) diblock copolymer; D = Kraton-*b*-poly(*n*BA)-*b*-Kraton triblock copolymer.

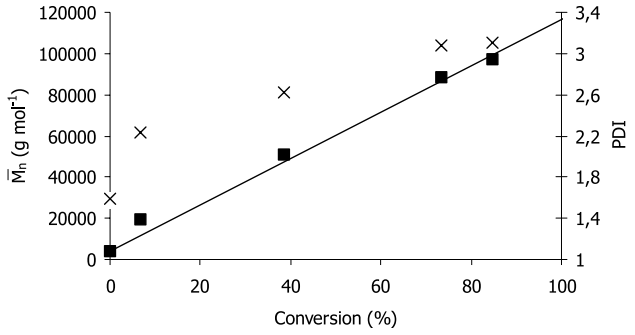

Fig. 9. Number average molar mass ($\bar{M}_n$, ■) and polydispersity index (PDI, ×) versus conversion for the miniemulsion polymerization of *n*BA, using a multifunctional 'poly(decyl-RAFT)' agent ($\bar{M}_{n,poly(decyl-RAFT)} = 3700$ g mol^{-1} in PS equivalents, $PDI_{poly(decyl-RAFT)} = 1.59$, on average 12 RAFT moieties present per molecule). Drawn line is the calculated $\bar{M}_n$. Average particle size diameter after polymerization: 207 nm.

desired triblock copolymer. The product that elutes at 15 min (GPC), which has the same elution time as the initial 'Kraton-RAFT' agent and therefore hinted to an incomplete consumption of the initially present 'Kraton-RAFT'agent, was shown to be di(Kraton)carbonate, which is an impurity that remained after the synthesis of this RAFT agent [16]. This conclusion could not be drawn from the GPC results described in Fig. 7, which clearly demonstrates the added value of a full MMCCD analysis. Furthermore, Kraton chloroformate was present in the mixture, responsible for the peak at a retention time of 16 min in Fig. 7. The relatively broad peak in the GPC chromatogram observed at 12–15 min represents overlapping peaks for di- and triblock copolymer, insufficiently separated by GPC but both visualized upon performing the MMCCD analysis, presented in Fig. 8. The relative amounts of the four components visible in the GPEC–GPC plot are: 70 ± 1 wt% Kraton–poly(*n*BA)–Kraton triblock copolymer (D), 20 ± 1 wt% Kraton–poly(*n*BA) diblock copolymer (C), 6 ± 1 wt% di(Kraton)carbonate (A), and 4 ± 1 wt% Kraton chloroformate (B). The presence of product B can, like the presence of di(Kraton)carbonate (A), be explained realizing that the RAFT agent was used without purification after its synthesis [16]. So, the total block copolymer yield is around 90 wt%, predominantly consisting of the desired triblock copolymer.

3.3. Polymerizations mediated with the 'poly(decyl-RAFT)' agent

Contrary to the 'Kraton-RAFT'/*n*BA mixtures (Section 3.2), a solution of the 'poly(decyl-RAFT)' in *n*BA remained homogeneous during the preparation of the miniemulsion under high shear conditions. Although traces of water must be introduced into the emulsion particles during the sonication, the 'poly(decyl-RAFT)'/*n*BA mixture does not phase separate. Fig. 9 shows $\bar{M}_n$ versus *n*BA conversion in the presence of the multifunctional 'poly(decyl-RAFT)' agent. For this homopolymerization of *n*BA, for which the conditions were comparable to those applied using the difunctional 'butyl-RAFT' agent, $\bar{M}_n$ increases linearly with conversion, indicating that also for this multifunctional RAFT agent the radical polymerization occurs in a controlled way and that the number of growing polymer chains is constant. This polymer shows a good match of the measured and calculated $\bar{M}_n$ value after 85% *n*BA conversion ($\bar{M}_{n,exp} = 97,000$ g/mol, $\bar{M}_{n,calc} = 99,500$ g/mol, PDI = 3.1). This relatively good match is thought to be a coincidence, since at least two counteracting phenomena (modified Mark–Houwink–Sakurada parameters due to the presence of several decyl and sulfur-containing residues in the main chain and possible loss and/or termination of RAFT functions) may operate simultaneously.

The poly(*n*BA) latex, obtained in the miniemulsion polymerization with the 'poly(decyl-RAFT)' agent, was used as a seed latex for the emulsion polymerization of *iso*-octyl acrylate (*i*OA). For this seeded emulsion polymerization the conditions were comparable to those used for the seeded emulsion polymerization described for the 'butyl-RAFT' agent. Also for this second step the experimentally determined $\bar{M}_n$ increased linearly with conversion, from 97,000 g/mol ($\bar{M}_{n,seed}$) to 152,000 g/mol for 90% *i*OA conversion, see Fig. 10. The calculated $\bar{M}_n$ was 178,000 g/mol. Here, obviously for PS calibration the presence of poly(*i*OA) blocks results in a less perfect match of calculated and experimental $\bar{M}_n$ values, as compared to the *n*BA based polymer described in Fig. 9. After the second polymerization step, the average particle size of the latex had increased from 207 to 302 nm.

The polymer obtained after 85% conversion in the first *n*BA polymerization step with $\bar{M}_{n,exp} = 97,000$ g/mol (Fig. 9), and the block copolymer obtained after the second polymerization step after an *i*OA conversion of 90% with $\bar{M}_{n,exp} = 152,000$ g/mol (Fig. 10) were submitted to complete base hydrolysis of the RAFT residues in the main

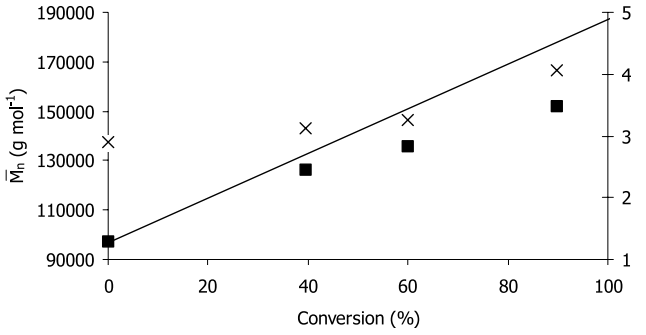

Fig. 10. Number average molar mass ($\bar{M}_n$, ■) and polydispersity index (PDI, ×) versus conversion for the seeded emulsion polymerization of *i*OA on the poly(*n*BA) seed latex, prepared using the 'poly(decyl-RAFT)' agent. Drawn line is calculated $\bar{M}_n$. Average particle size diameter after polymerization: 302 nm.

chain, namely by a treatment with triethylamine in a water/DMF mixture at 90 °C for 48 h. After careful analysis of the hydrolysis products by SEC and gradient polymer elution chromatography, using a solvent gradient from 85/15 water/THF (wt/wt) to pure THF in 20 min, it turned out that the molar mass of the polymer obtained after the first polymerization step had been reduced to a number-average molar mass of 18,900 g/mol. The observed reduction of $\bar{M}_n$ implies that before hydrolysis on average about five (97,000/18,900) poly(*n*BA) blocks were present in the product. Complete hydrolysis of the polymer obtained after the second polymerization step, which due to the nature of the RAFT process will always yield an ABA triblock or a mixture of diblock and triblock copolymers, resulted in a decrease of the molar mass from 152,000 to 46,800 g/mol. The fact that the polymer blocks obtained after base hydrolysis had a higher molar mass after the second polymerization step than after the first step, clearly shows that a multiblock copolymer has been formed upon insertion of the *i*OA monomer into the end product of the first polymerization step. These blocks must contain both *n*BA and *i*OA monomer residues. A rough calculation demonstrates that the end product, of the experiment on which Fig. 10 is based, consisted (on average) of about three (152,000/46,800) p(*i*OA)-*block*-pBA(-*block*-p(*i*OA)) di- and/or triblock copolymers. The reason that the number of blocks is significantly lower than expected from the initial number of RAFT groups present in the multifunctional RAFT agent, is that not all main chain scissions, occurring during the fragmentation step, are restored later on. Some growing chain radicals are irreversibly terminated. This phenomenon is valid for all polymerizations using the di- and multifunctional RAFT agents described in this paper, which obviously is responsible for the relatively broad molar mass distributions observed in Figs. 1, 2, 6, 9 and 10. This process can probably be limited by raising the RAFT agent/free radical initiator ratio. The PDI of the copolymers generated using the 'poly(decyl-RAFT)' agent (Figs. 9 and 10) is further raised by the relatively high PDI of this multifunctional RAFT agent itself (PDI = 1.59, see Ref. [16] and Fig. 9). Obviously, this latter broadening effect can be limited or even prevented by fractionation of the synthesized 'poly(decyl-RAFT)' agent.

4. Conclusions

We have demonstrated that multifunctional RAFT agents, depending on the number of RAFT groups they contain, yield tri- or even multiblock copolymers in merely two polymerization steps in a miniemulsion polymerization process. If macromolecular difunctional RAFT agents are used, in which one type of polymeric blocks is already present, then one polymerization step yields a triblock copolymer. The number of blocks generated in the (multi)-block copolymers is lower than expected in view of the number of RAFT groups in the multifunctional RAFT agent, and the experimental molar mass only occasionally agrees with the theoretically expected value. These issues can probably be solved by optimizing the flux of radicals into the latex particles.

So, although the degree of control of the number of blocks and of the molar mass of the blocks in the copolymer requires optimization, the enormous versatility of the described concept allows quick production of segmented block copolymers in a relatively simple emulsion polymerization process. The multiblock copolymer latex product may find application as e.g. pressure sensitive adhesives.

Acknowledgements

The authors acknowledge the help of our colleagues Marion van Straten, Henk Claessens, Bastiaan Staal, Michal Halama and Wieb Kingma with the MALDI-TOF-MS and the GPEC–GPC analyses. Prof Oren Regev of the Ben-Gurion University of the Negev is acknowledged for the cryo-TEM pictures. UCB Chemicals is acknowledged for the gift of *iso*-octyl acrylate, and we are grateful to Kraton BV for the gift of Kraton L-1203.

References

[1] Chiefari J, Chong YK, Ercole F, Krstina J, Jeffery J, Le TPT, et al. Macromolecules 1998;31:5559.
[2] Le TPT, Moad G, Rizzardo E, Thang SH. PCT Int Appl, WO 9801478 to DuPont; 1998.
[3] Chiefari J, Mayadunne RTA, Moad G, Rizzardo E, Thang SH. PCT Int Appl, WO 9931144 to DuPont; 1999.
[4] Chong YK, Le TPT, Moad G, Rizzardo E, Thang SH. Macromolecules 1999;32:2071.
[5] Convertine AJ, Sumerlin BS, Thomas DB, Lowe AB, McCormick CL. Macromolecules 2003;36:4679.

[6] Vasilieva YA, Thomas DB, Hennaux PE, McCormick CL. Polym Prepr 2003;44:886.
[7] Donovan MS, Sanford TA, Lowe AB, Sumerlin BS, Mitsukami Y, McCormick CL. Macromolecules 2002;35:4570.
[8] Severac R, Lacroix-Desmazes P, Boutevin B. Polym Int 2002;51:1117.
[9] Krstina J, Moad G, Rizzardo E, Winzor CL. Macromolecules 1995; 28:5381.
[10] De Brouwer H. RAFT memorabilia, living radical polymerization in homogeneous and heterogeneous media. PhD Thesis. Eindhoven, The Netherlands; 2001.
[11] Smulders W. Macromolecular architecture in aqueous dispersions, living free radical polymerization in emulsion. PhD Thesis. Eindhoven, The Netherlands; 2002.
[12] Pham BTT, Nguyen D, Ferguson CJ, Hawkett BS, Serelis AK, Such CH. Macromolecules 2003;36:8907.
[13] Destarac M, Charmot D, Franck X, Zard SZ. Macromol Rapid Commun 2000;21:1035.
[14] Chiefari J, Mayadunne RTA, Moad CL, Moad G, Rizzardo E, Postma A, et al. Macromolecules 2003;36:2273.
[15] Corpart P, Charmot D, Zard SZ, Franck X, Bouhadir G. PCT Int Appl, WO 9935177 to Rhodia; 1999.
[16] Bussels R, Koning CE. Tetrahedron 2005;61:1167–73. Bussels R, Bergman-Göttgens C, Meuldijk J, Koning C. Macromolecules 2004; 37:9299.
[17] Higaki Y, Otsuka H, Endo T, Takahara A. Macromolecules 2003;36: 1494.
[18] Motokucho S, Sudo A, Sanda F, Endo T. Chem Commun 2002;1946.
[19] You YZ, Hong CY, Pan CY. Chem Commun 2002;2800.
[20] Almgren M, Edwards K, Karlsson G. Colloids Surf A: Physicochem Eng Aspects 2000;174:3–21.